JOURNAL OF MATERIALS SCIENCE 22 (1987) 1271–1276

Fracture toughness measurements in ceramics: pre-cracking in cyclic compression

S. SURESH, L. EWART, M. MADEN, W. S. SLAUGHTER, M. NGUYEN
Division of Engineering, Brown University, Providence, Rhode Island 02912, USA

Experimental observations of stable Mode I fatigue crack growth at room temperature in notched plates of brittle solids subjected to fully compressive far-field cyclic loads have recently been reported. In this paper, we outline an experimental procedure whereby the fracture toughness and R-curves for ceramics can be determined in bending (or tension) after pre-cracking notched specimens in uniaxial cyclic compression to produce a controlled and through-thickness fatigue flaw. The capability of this technique to provide reproducible fracture toughness values is illustrated with the aid of experimental results obtained for coarse-grained and fine-grained aluminium oxide.

1. Introduction

The measurement of fracture toughness for brittle materials is an inherently difficult task. The principal obstacle in the determination of reliable values of critical fracture parameters in brittle solids is the experimental problem associated with introducing a sharp, through-thickness crack prior to quasi-static fracture testing. Unlike metallic materials, brittle solids such as ceramics are known to undergo catastrophic failure with little or no stable crack growth at room temperature under fully or partly tensile cyclic loads. Therefore, traditional approaches to the development of fracture test methods for ceramics have focused on specimen designs which circumvent the need for a fatigue pre-crack or artificially induce a certian amount of stable crack growth during quasi-static loading. To date, however, no standardized fracture toughness test or specimen geometry has been established for ceramic materials, although a wide variety of methods have been proposed and investigated (e.g. [1]). Some currently practised techniques for fracture testing of brittle materials include the simple notched bend bar method (e.g. [2, 3]), the chevron V-notched short rod or bar methods [4, 5], (Palmqvist) indentation techniques [6, 7] and the bridge compression method [8, 9].

An approximate measure of fracture toughness is generally obtained for ceramics using notched specimens quasi-statically fractured in three-point or four-point bending without any "sharp" pre-crack (e.g. [2, 3, 10]). It is, however, well known that fracture toughness measured or inferred from this procedure can be markedly influenced by the artifacts of the notch geometry (e.g. [3]). *Non-conservative* estimates of critical fracture parameters can result from this method because of the finite radius of the notch-root. The chevron V-notched short rod or bar specimens promote stable crack growth during the quasi-static fracture test and the critical stress intensity factor, K_{Ic}, is calculated based on the maximum load observed during the test [4, 5]. This procedure thus circumvents the need for introducing a fatigue pre-crack prior to fracture toughness measurements and promotes high constraint at the crack front. Although expensive specimen preparation is necessary to produce the intricate chevron notch geometry, the short-rod method is gaining increasing popularity because of its capability to produce a fracture toughness estimate after stable crack advance. There is, however, evidence indicating that the fracture toughness value measured using this technique may depend on the specimen geometry and initial crack length in some materials [11, 12]. Furthermore, this method is generally not considered suitable for monitoring the changes in crack growth resistance with crack advance (i.e. for measuring resistance curves) [13].

In the (Vickers) indentation method, Palmqvist or semi-circular median pre-cracks are introduced into the specimen by the indentor [6, 7, 14]. This method, however, is fraught with difficulties which stem from the fact that a zone of plastically deformed material forms at the base of the indentor. This damage incurred by the test specimen can substantially affect subsequent fracture toughness measurements [14]. Moreover, crack branching/multiple cracking may restrict the validity of such measurements in certain materials [15]. Length measurements for surface cracks formed during indentation are also prone to considerable inaccuracies. In the "bridge" compression method, a Vickers hardness indentation is made centrally on the top surface of a rectangular bar specimen [8]. Following this, the specimen is supported on an anvil and compressed with two rectangular punches, one on each side of the indentation. The geometry of the specimen promotes a maximum tensile stress at the top surface which diminishes with increasing distance into the specimen, eventually becoming compressive after a certain depth [9]. The bridge compression cracks form at the corners of the indentation to extend into a straight through-thickness flaw that can be used for K_{Ic} measurement in a bend specimen The artefacts of the geometrical and

0022–2461/87 $03.00 + .12

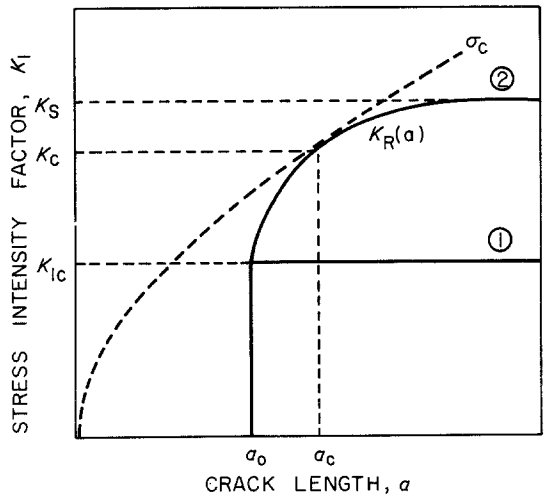

Figure 1 Schematic representation of variation of stress intensity factor with crack length; Curve 1 illustrates catastrophic failure with no stable crack growth; Curve 2 is a schematic plot of the resistance curve behaviour associated with "toughened" ceramics. See text for details.

load variables as well as the extent of residual damage left at the tip of the sharp flaw produced by this method (at lower temperatures) are known to affect subsequent fracture toughness measurements [16]. Furthermore, this relatively new method has not yet been investigated thoroughly. In view of the limitations associated with the various fracture testing methods currently available for brittle solids, there is a continuing research effort to explore novel test procedures for the measurement of critical fracture properties.

In addition to determining the critical stress intensity factors for fracture *initiation* (i.e. K_{Ic}), there is a growing interest in monitoring the progressive changes in crack growth resistance during *stable* quasi-static fracture in toughened ceramics which are being developed for potential structural applications. The resistance of ceramics to crack growth under quasi-static loads can be enhanced by intrinsic and extrinsic toughening mechanisms involving crack deflection, microcracking, crack bridging and phase transformations [17]. The increase in apparent fracture toughness with quasi-static crack growth is a property of particular interest for many structural ceramics. Fig. 1 schematically shows the stress intensity factor against crack length plots for quasi-brittle materials (Curve 1) and for materials exhibiting stable crack growth during quasi-static fracture (Curve 2, known as the R-curve). Fine-grained, single-phase ceramics typically exhibit catastrophic fracture, similar to the behaviour depicted by Curve 1, at a critical stress intensity factor K_{Ic}. However, transformation-toughened ceramics are known to exhibit considerable subcritical crack growth, similar to the behaviour illustrated by Curve 2, prior to final fracture [18]. The heavy dashed line in Fig. 1 represents the schematic variation of the applied stress intensity factor K_I with crack length, a, (i.e. according to the relationship K_I = constant $\sigma_c a^{1/2}$) at a constant applied stress σ_c. K_c is the stress intensity factor presenting the onset of unstable equilibrium. Below K_c, the rate of increase of material fracture resistance with crack length ($K_R(a)$) is greater than the rate of increase in applied K_I with crack length. This leads to stable crack growth. Above K_c, however, the reverse situation is prevalent and hence catastrophic fracture results. The slope of the transient region of the R-curve, between the fracture initiation toughness K_{Ic} and the point of catastrophic failure K_s, thus provides a measure of toughening during stable crack growth. The generation of "valid" R-curves for toughened ceramics is also somewhat restricted by the experimental difficulties in introducing a sharp fatigue pre-crack prior to the quasi-static fracture test. Where R-curves have been directly measured in notched bend specimens or using indentation techniques, it is found that the depth and root radius of the notch or prior damage induced in the specimen can significantly affect the slope of the R-curve [3, 19]. This leads to considerable uncertainty in interpreting the beneficial effects of a particular toughening mechanism. An ideal solution to this problem would be the development of experimental capabilities, analogous to the case of metals, to introduce a "sharp" through-thickness fatigue pre-crack in a simple fracture specimen, prior to the measurement of quasi-static fracture toughness or R-curves.

In a recent paper, Ewart and Suresh [20] reported experimental observations of stable, Mode I fatigue crack growth in notched plates of polycrystalline alumina subject to fully compressive cyclic loads at room temperature. The fatigue cracks propagate at a progressively decreasing velocity along the plane of the notch (in a direction macroscopically normal to the compression axis) and arrest completely. It was suggested that this method of introducing a *stable* and *self-arresting* fatigue flaw in a simple edge-notched specimen would provide a new possibility for measuring the fracture properties of brittle materials [20, 21] The micromechanisms of crack advance from notches under far-field cyclic compression were discussed in detail [21]. As shown by Suresh and co-workers [20–24], the phenomenon of crack growth under cyclic compressive stresses exhibits a macroscopically similar behaviour in a wide range of materials spanning the very ductile metals to extremely brittle solids, although the mechanisms underlying this effect are very different among the various classes of materials. A characteristic feature of this phenomenon which is common to all cases is that the *local* zone of damage is fully encompassed by material elastically strained in compression so that crack growth is stable and non-catastrophic. There is some experimental evidence which indicates that the maximum amount of damage left at the tip of the fatigue crack propagated (until self-arrest) under far-field cyclic compression is not large enough to affect subsequent fracture measurements in tension or bending [24].

The objective of this paper is to show that crack initiation under cyclic compression can be used as a pre-cracking technique for measuring fracture initiation toughness K_{Ic} and R-curves in ceramics. We present experimental results of fracture toughness measurements in fine-grained (range of grain sizes = 1 to 6 μm, average grain size = 3 μm) and coarse-

TABLE I Properties of material studied

Property	Material	
	AD 995	AD 999
Al_2O_3 (%)	99.5	99.9
Specific gravity	3.89	3.96
Grain size		
Average (μm)	17	3
Range (μm)	5 to 50	1 to 6
Compressive strength at 25° C (MPa)	2620	3792
Flexural strength at 25° C (MPa)	379	552
Tensile strength at 25° C (MPa)	262	310
Modulus of elasticity (GPa)	372	386
Impurities and grain-boundary phases	SiO_2, MgO, Ca, Na, Fe	

grained (range of grain sizes = 5 to 50 μm, average grain size = 17 μm) aluminium oxide to illustrate the feasibility of this technique for fracture testing in ceramics. The change in stress intensity factor as a function of crack advance was also examined in these experiments to check the postulates of the microcrack-toughening theories that the coarse-grained Al_2O_3 specimen may exhibit stable crack growth (R-curve) during quasistatic fracture [3, 25]. The advantages and limitations of the compression fatigue method are highlighted.

2. Materials and experimental methods

Fatigue cracks were introduced in single-edge-notched specimens of 99.5% and 99.9% pure polycrystalline alumina cycled under compression–compression fatigue loads. These materials are commercially available as grade AD 995 and AD 999, respectively, from Coors Porcelain Co., Boulder, Colorado. The properties of the two materials are listed in Table I. A single-edge notch, with a root radius of about 0.5 mm, was introduced in the specimens using a diamond wheel. Fig. 2 schematically shows the specimen geometry used in the fracture experiments. The fatigue crack

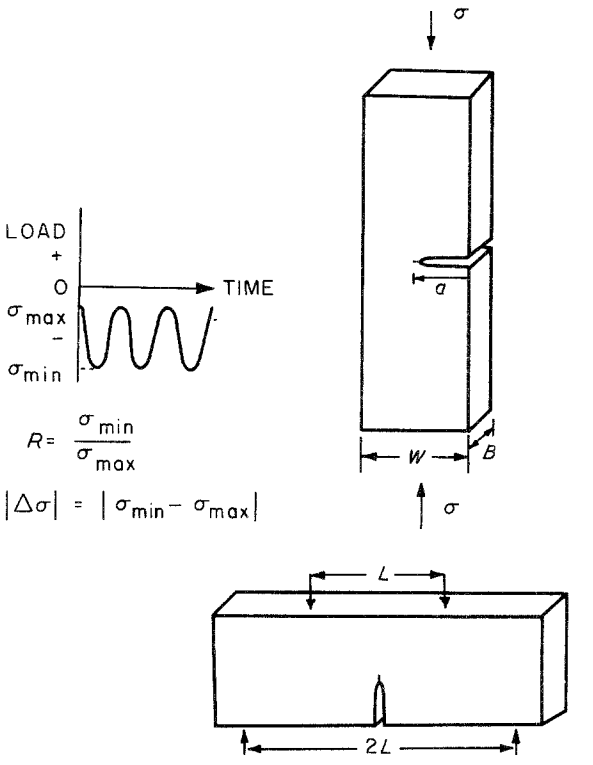

Figure 2 Schematic representation of the procedure for pre-cracking in uniaxial cyclic compression and subsequent quasi-static fracture in four-point bending.

was introduced in uniaxial cyclic compression (Fig. 2a) and subsequently quasi-static fracture tests were conducted in four-point bending (Fig. 2b). A total of eight fracture toughness tests were conducted and the procedure followed was identical for both the materials. The actual dimensions of the specimens are described in Table II. All experiments were conducted in the laboratory environment at a temperature of about 22° C and relative humidity of about 40%. The fatigue pre-cracks were introduced in uniaxial cyclic compression at a loading frequency of 20 Hz with a sinusoidal waveform and a load ratio, R = 10. The load ratio is defined as the ratio of the minimum load to the maximum load of the fatigue cycle (Fig. 2a).

TABLE II Results of fracture toughness tests on polycrystalline alumina

Variable	AD 995 Al_2O_3						AD 999 Al_2O_3	
	Type A tests*			Type B tests†			Type B tests†	
	Specimen 1	Specimen 2	Specimen 3	Specimen 4	Specimen 5	Specimen 6	Specimen 7	Specimen 8
Dimensions‡								
a (mm)	6.36	5.44	5.62	5.35	5.60	5.02	5.66	5.69
W (mm)	15.93	10.34	10.50	10.39	10.38	10.01	10.40	10.40
B (mm)	5.31	5.11	5.11	6.41	6.40	6.40	6.36	6.50
a/W	0.40	0.53	0.54	0.51	0.54	0.50	0.54	0.55
Fracture toughness results								
K_{Ic} (MPa $m^{1/2}$): equations from								
Krause and Fuller [26]	4.24	4.40	4.68	3.90	5.12	4.09	3.25	3.66
Dong [27]§	4.22	4.37	4.65	3.87	5.08	4.06	3.23	3.64
Kavishe [26]	4.23	4.39	4.67	3.89	5.11	4.08	3.24	3.66

*Type A refers to specimens where the side surfaces were ground after pre-cracking in cyclic compression to eliminate crack front non-uniformity.

†Type B refers to specimens where fracture toughness in bending was measured directly after pre-cranon-uniformity.

†Type B refers to specimens where fracture toughness in bending was measured directly after pre-cracking in cyclic compression.

‡The inner span in the four-point bend test, $L \approx 2W$, for all specimens.

§Dong's K_I calibration for four-point bend specimens is within 0.6% of the result derived by Brown and Srawley [29] for $0.2 \leqslant a/w \leqslant 0.6$.

Compressive stress ranges $|\Delta\sigma|$ of about 305 and 410 MPa were required to pre-crack the AD 995 and AD 999 materials, respectively. The specimens were located between two parallel plates during compression fatigue. The alignment between the plates was ensured with the aid of guide pins. A fatigue crack about 0.4 mm in length was detected within the first 30 000 cycles in all the experiments. The crack mouth opening displacement was monitored with the aid of the clip gauge mounted between knife edges cemented to the specimen. The crack length was also monitored with the aid of an optical microscope.

It was reported by Ewart and Suresh [20] that very near the unconstrained side surfaces of the edge-notched specimen, a slight non-uniformity in crack front may occur during pre-cracking in cyclic compression. The crack length within about 0.5 mm of the side surfaces was found to be somewhat larger than that in the interior of the specimen [20]. In order to evaluate the possible effects of this small non-uniformity in crack front, we conducted the following two types of experiments. In one set of experiments (Type A), about 0.5 mm was ground from each of the two side surfaces after pre-cracking cyclic compression. This enabled us to ensure that the crack front was straight through the thickness of the specimen during the fracture toughness test. All the dimensions shown in Table II refer to the final specimen geometry during the quasi-static fracture experiments. In the second set of experiments (Type B), the quasi-static bend tests were performed directly after pre-cracking in uniaxial cyclic compression.

3. Results and discussion

Fig. 3 shows an optical micrograph of the Mode I fatigue crack at the root of the notch (in Specimen 5) observed on the specimen surface after about 15 000 cycles of uniaxial compression loading. An example of the fatigue crack front (Type B) resulting from such an experiment is illustrated in Fig. 4. Here, the fatigue crack front is denoted by A at the side surface and by C at the interior of the specimen. This optical micrograph of the fracture surface reveals that the crack front is uniformly straight in the interior section of the specimen (e.g. location C), whereas slightly faster crack growth occurs within about 0.5 mm of the unconstrained side surface (location A) in the 6.4 mm thick specimens. Fig. 5 shows an example of the fatigue crack front in Type A specimens where the length of the fatigue crack was the same through the entire thickness. In this case, the slight non-uniformity in crack front near the side surfaces was eliminated by removing a 0.5 mm thick layer of material on either side by a grinding operation after fatigue pre-cracking in compression.

The fracture toughness values, K_{Ic}, for the four-point bend specimens were calculated using three different stress intensity factor solutions published in the literature [26–28]. The formulae used in these calculations are described in the Appendix. Table II shows all the results of the fracture toughness calculations for AD 995 and AD 999 polycrystalline alumina bend

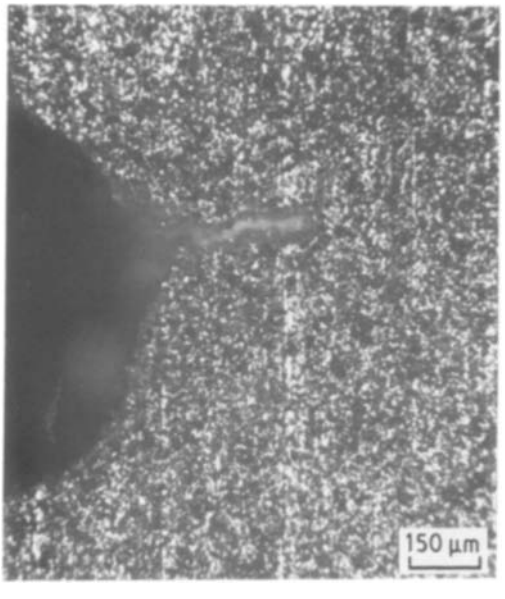

Figure 3 Mode I fatigue crack in the single-edge-notched specimen loaded in uniaxial cyclic compression. Load in vertical direction. The compression axis is in vertical direction.

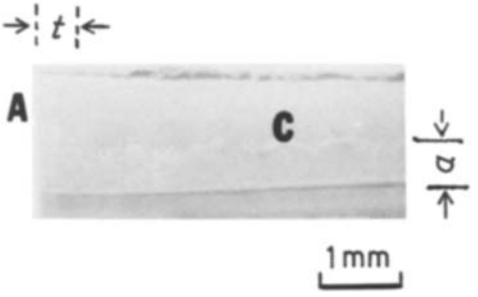

Figure 4 An optical micrograph of the fracture surface in a Type B specimen of AD 995 Al_2O_3 showing a fatigue crack of length, a, at the tip of the notch (at the bottom of the figure). Note the larger crack growth distance at the near-surface location A (over a distance $t \approx 0.5$ mm) than in the interior thickness location C.

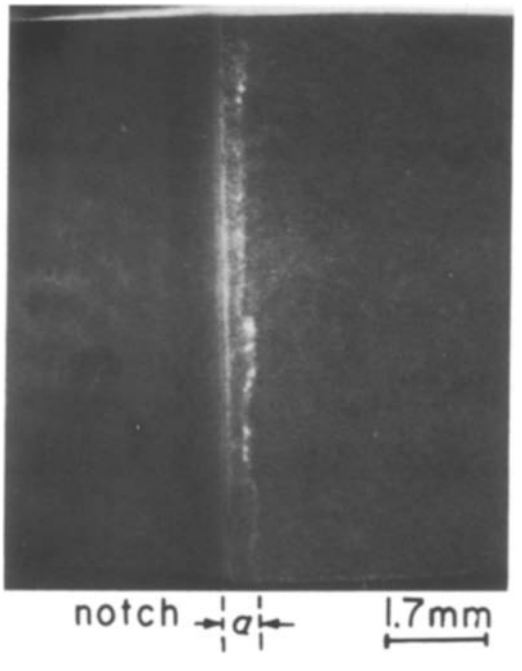

Figure 5 A straight, through-thickness Mode I fatigue pre-crack in the Type A specimen.

specimens. The following conclusions can be drawn from the results shown in Table II:

1. Reproducible fracture toughness measurements can be obtained using the cyclic compression method for pre-cracking ceramics.

2. Type B specimens exhibit relatively more scatter in K_{Ic} than Type A specimens. However, the difference in fracture toughness between Type A and Type B specimens of AD 995 was within the normal range of experimental variability observed for ceramics. This seems to indicate that any small non-uniformity in fatigue crack front very near the side surfaces does not significantly affect the fracture toughness.

3. As expected (e.g. [25]), the finer-grained AD 999 (average $K_{Ic} \approx 3.45\,\text{MPa}\,\text{m}^{1/2}$) material has a lower fracture toughness than AD 995 (average $K_{Ic} \approx 4.4\,\text{MPa}\,\text{m}^{1/2}$).

4. The materials examined in this work did not exhibit detectable stable crack growth during quasi-static fracture (within the resolution, about 0.04 mm, of crack length measurements). Hence, the stress intensity factor (K_I) against crack length (a) plot (R-curve) has a zero slope after the onset of fracture in both the materials (Curve 1 in Fig. 1).

5. The different solutions for stress intensity factor calculations provide about the same value of K_{Ic} for both the materials.

Some prior studies of quasi-static fracture in notched bend specimens of coarse-grained, single-phase Al_2O_3 have indicated the possibility of stable crack growth and the existence of R-curves [3, 19]. Although the slope of the R-curve was found to be very strongly affected by the geometry of the notch in these specimens fracture-tested without a sharp pre-crack, the occurrence of stable crack growth due to grain-boundary microcracking was postulated. Our experiments on quasi-static fracture in notched bend specimens containing a fatigue pre-crack do not indicate a clearly noticeable R-curve effect (within the resolution of crack length detection) even in the coarse-grained AD 995 Al_2O_3 with a grain size range of 5 to 50 μm and average grain size of 17 μm. Further work, using the compression fatigue pre-cracking method, is required in a variety of materials exhibiting a wider range of grain sizes before the possible beneficial effects of crack-tip shielding due to the microcrack toughening mechanism can be fully evaluated. However, the present results do underscore the need to exercise caution in estimating the improvements in toughness based on fracture experiments performed in bend specimens containing blunt notches [3, 19] or pre-cracks produced by indentation [15].

Following the compression technique described earlier [20, 21], we have demonstrated in this work that reproducible K_{Ic} values can be obtained for ceramics in edge-notched specimens fatigue pre-cracked in cyclic compression. The introduction of a fatigue pre-crack in notched plates of polycrystalline ceramics under cyclic compression offers some unique advantages for fracture toughness and R-curve measurements:

1. Controlled and non-catastrophic fatigue cracks can be obtained in brittle materials even at room temperature.

2. Fracture toughness and resistance curves can be measured using simple edge-notched/bend specimens.

3. Since the specimen is loaded under fully compressive stresses, no specialized (tensile) grips are needed to load the specimen.

4. The total distance of crack growth under far-field cyclic compression can be suitably manipulated by controlling the load amplitude, load ratio and notch geometry.

5. This method offers the possibility of obtaining the resistance curves for ceramics from fatigue pre-cracks similar to the procedures employed for metals. Therefore, the intrinsic effects of toughening by transformation, deflection or microcracking during stable crack growth can be investigated with the shape of the resistance curves likely to be unaffected by the specimen geometry.

6. The local zone of damage during cyclic compression is fully embedded in material elastically strained in far-field compression. Thus the process of pre-cracking is intrinsically stable. As the crack decelerates and arrests naturally, the maximum extent of damage left at the tip of the crack grown (until arrest) under far-field cyclic compression is not likely to affect subsequent fracture tests in tension or in bending. Although further work is needed to fully substantiate this hypothesis, our related studies have shown that the same fracture behaviour in bending can be obtained following pre-cracking at different cyclic compressive load levels. This result is especially important for ceramics toughened by crack-shielding mechanisms where a minimum "process zone" is desirable at the tip of a notch or a pre-crack prior to fracture toughness measurements.

The advantages of the compression fatigue method as a pre-cracking scheme for ceramics are borne out by the experimental results obtained in this work. We emphasize, however, that there are several aspects of this technique which warrant extensive further investigation in a wide variety of materials before it can be routinely employed in fracture property measurements for ceramics. The effects of notch geometry, specimen geometry, microstructure (especially composition, grain size and grain-boundary glassy phases) and environment on the characteristics of fatigue crack growth in cyclic compression should be evaluated thoroughly. Further work is also needed to document the effect of damage at the tip of the fatigue pre-crack initiated in compression and its effects on subsequent fracture measurements, especially in ceramics toughened by phase transformations and microcracking. It should also be noted that pre-cracking in cyclic compression does not appear to be feasible in single crystals of ceramics where only catastrophic "splitting" parallel to the compression axis is observed [21].

Subsequent to the conclusion of the present work, Tschegg and Suresh [30] conducted fracture toughness tests for ceramics in uniaxial tension. Circumferentially-notched cylindrical rods of a polycrystalline

Al_2O_3 were pre-cracked in cyclic compression to introduce a concentric fatigue flaw (following the technique employed in this study). Subsequently, the pre-cracked rods were fractured in pure tension. Highly reproducible values of fracture toughness were obtained using this method [30].

4. Conclusions

A novel experimental technique for the measurement of fracture toughness and R-curves in ceramics has been demonstrated. In this method, a fatigue pre-crack is introduced in single-edge-notched specimens loaded in uniaxial cyclic compression. Subsequently, the specimen containing the fatigue flaw can be fractured in bending or in tension. Reproducible values of fracture toughness are obtained using this method in two grades of single-phase polycrystalline aluminium oxide. While the scatter in the measured toughness values is generally low in all the tests, Type A specimens (where the linearity of the fatigue crack front was fully ensured) exhibit the least variability in fracture toughness. The proposed technique offers some interesting possibilities for measuring fracture initiation toughness and R-curves (from fatigue pre-cracks) in ceramics toughened by crack shielding mechanisms. Further work is needed to evaluate the influence of pre-cracking in compression fatigue and of specimen geometry on subsequent measurements of fracture properties in toughened ceramics.

Acknowledgements

This work was supported by the National Science Foundation under Grant NSF-ENG-8451092. The use of Central Mechanical Testing Facilities of the Materials Research Laboratory at Brown University is gratefully acknowledged. The authors thank Mr Chris Bull for his help during the course of this work.

Appendix

The critical stress intensity factor, K_{Ic}, for the four-point bend specimens of polycrystalline Al_2O_3 (Table II) was calculated from three different solutions available in the literature. The specimen dimensions a, W, B and L ($\approx 2W$) are schematically illustrated in Fig. 2. P is the applied load and $\boldsymbol{a} = a/W$. From Kavishe [26],

$$K_I = \frac{P}{B(W)^{1/2}}(5.96\boldsymbol{a}^{1/2} - 7.39\boldsymbol{a}^{3/2} + 38.92\boldsymbol{a}^{5/2} - 69.66\boldsymbol{a}^{7/2} + 74.44\boldsymbol{a}^{9/2}) \quad \text{(A1)}$$

for $0.3 \leqslant \boldsymbol{a} \leqslant 0.6$.

From Dong [27],

$$K_I = \frac{PL}{4BW^{3/2}}(0.8\boldsymbol{a}^{1/2} + 3.524\,(1 - \boldsymbol{a})^{-1.59}) \quad \text{(A2)}$$

for $0.2 \leqslant \boldsymbol{a} \leqslant 0.6$. For this range of $\boldsymbol{a}$, the results of Dong [27] are within 0.6% of the formula derived by Brown and Srawley [29].

After Krause and Fuller [28],

$$K_I = \frac{P}{BW^{1/2}}\left[1.5\left(\frac{L}{W}\right)\boldsymbol{a}^{1/2}(1 - \boldsymbol{a})^{-3/2}\right] \times [1.9887 - 1.326\boldsymbol{a} - (3.49 - 0.68\boldsymbol{a} + 1.35\boldsymbol{a}^2) \times \boldsymbol{a}(1 - \boldsymbol{a})(1 + \boldsymbol{a})^{-2}] \quad \text{(A3)}$$

for $0 < \boldsymbol{a} < 1$.

References

1. R. WARREN and H. MATZKE, in "Science of Hard Metals", edited by R. Viswanadham and J. Gurland (Plenum Press, New York, 1984) p. 631.
2. M. V. SWAIN and R. H. J. HANNINK, "Advances in Ceramics", Vol. 12, edited by N. Claussen, M. Riihle and A. H. Heuer (American Ceramic Society, Columbus, Ohio, 1984) p. 225.
3. R. KNEHANS and R. STEINBRECH, *J. Mater. Sci. Lett.* **1** (1982) 327.
4. L. M. BARKER, *Eng. Fract. Mech.* **9** (1977) 361.
5. D. MUNZ, R. T. BUBSEY and J. E. SRAWLEY, *Int. J. Fract.* **16** (1980) 359.
6. B. R. LAWN and T. R. WILSHAW, *J. Mater. Sci.* **10** (1975) 1049.
7. A. G. EVANS and T. R. WILSHAW, *Acta Metall.* **24** (1976) 939.
8. T. SADAHIRO and S. TAKATSU, *Modern Dev. Powder Metall.* **14** (1980) 561.
9. R. WARREN and B. JOHANNESSON, *Powder Metall.* **27** (1984) 25.
10. M. V. SWAIN, in "Fracture Mechanics of Ceramics", Vol. 6, edited by R. C. Bradt, A. G. Evans, D. P. H. Hasselman and F. F. Lange (Plenum Press, New York, 1983) p. 355.
11. J. L. SHANNON Jr. and D. G. MUNZ, ASTM STP 855 (American Society for Testing and Materials, Philadelphia, 1984) p. 270.
12. A. R. INGRAFFEA, K. L. GUNSALLUS, J. F. BEECH and P. P. NELSON, ASTM STP 855 (American Society for Testing and Materials. Philadelphia, 1984) p. 152.
13. J. C. NEWMAN Jr, ASTM STP 855 (American Society for Testing and Materials, Philadelphia, 1984) p. 5.
14. D. B. MARSHALL and A. G. EVANS, *J. Amer. Ceram. Soc.* **64** (1981) C182.
15. G. R. ANSTIS, P. CHANTIKUL, B. R. LAWN and D. B. MARSHALL, *ibid.* **64** (1981) 533.
16. R. GODSE, MS thesis, Brown University (1985).
17. A. G. EVANS, A. H. HEUER and D. L. PORTER, in "Fracture 1977", edited by D. M. R. Taplin (University of Waterloo Press, Waterloo, 1977) p. 529.
18. R. M. McMEEKING and A. G. EVANS, *J. Amer. Ceram. Soc.* **65** (1982) 242.
19. R. STEINBRECH, paper presented at the 88th Annual Meeting of American Ceramic Society, Chicago, April 1986 (unpublished).
20. L. EWART and S. SURESH, *J. Mater. Sci. Lett.* **5**(8) (1986) 774.
21. *Idem, J. Mater. Sci.* in press.
22. S. SURESH, *Eng. Fract. Mech.* **21** (1985) 453.
23. S. SURESH and L. A. SYLVA, *Mater. Sci. Eng.* **83** (1986) L7.
24. S. SURESH, T. CHRISTMAN and C. BULL, in "Short Fatigue Cracks," edited by R. O. Ritchie and J. Lankford (The Metallurgical Society of AIME, Warrendale, Pennsylvania, 1986) p. 513.
25. Y. FU, PhD thesis, University of California (1983).
26. F. P. L. KAVISHE, *Int. J. Fract.* **27** (1985) R13.
27. F. DONG, *ibid.* **24** (1984) R107.
28. R. F. KRAUSE and E. R. FULLER, ASTM STP 855 (American Society for Testing and Materials, Philadelphia, 1984) p. 309.
29. W. F. BROWN and J. E. SRAWLEY, ASTM STP 410 (American Society for Testing and Materials, Philadelphia, 1966) p. 32.
30. E. K. TSCHEGG and S. SURESH, *Comm. Amer. Cer. Soc.* **70** (1987) in press.

Received 19 May
and accepted 23 July 1986